Journal of the Korean Magnetic Resonance Society **2018**, *22*, 18-25
DOI 10.6564/JKMRS.2018.22.1.018

Backbone Dynamics and Model-Free Analysis of N-terminal Domain of Human Replication Protein A 70

Sooji Yoo and Chin-Ju Park*

Department of Chemistry, Gwangju Institute of Science and Technology, Gwangju 61005, South Korea

Received Jan 30, 2018; Revised Feb 20, 2018; Accepted Mar 4, 2018

Abstract
Replication protein A (RPA) is an essential single-stranded DNA binding protein in DNA processing. It is known that N terminal domain of RPA70 (RPA70N) recruits various protein partners including damage-response proteins such as p53, ATRIP, Rad9, and MRE11. Although the common binding residues of RPA70N were revealed, dynamic properties of the protein are not studied yet. In this study, we measured ^{15}N relaxation parameters (T_1, T_2 and heteronuclear NOE) of human RPA70N and analyzed them using model-free analysis. Our data showed that the two loops near the binding site experience fast time scale motion while the binding site does not. It suggests that the protein binding surface of RPA70N is mostly rigid for minimizing entropy cost of binding and the loops can experience conformational changes.

Keywords RPA70N, NMR, backbone dynamics, model-free analysis, reduced spectral density mapping

Introduction

Replication protein A (RPA) is an essential single-stranded (ss) DNA binding protein (SSB) which is conserved in eukaryotes for DNA processing such as replication, repair, and recombination. It protects DNA from nuclease, inhibits the formation of the hairpin, and regulates reannealing until DNA processing is completed.[1-8] In these functions, RPA interacts with ssDNA and other proteins involved in DNA metabolism in response to DNA damage. Interactions are modulated by their different affinity levels inducing a conformational change of RPA.[1–15]

RPA is a stable heterotrimer consisted of three subunits (70, 32, and 14 kDa). There is one winged helix-turn-helix fold domain (RPA32C) and six oligonucleotides/oligosaccharide binding (OB)-fold domains (RPA70N, A, B, C, RPA32D and RPA14) common to SSBs.[8,16,17] RPA32D, RPA14 and N-terminal domain of RPA70 (RPA70N) primarily functions as protein-protein interaction modules but also has weak ssDNA binding affinity. They specifically interact with transcription factors and DNA polymerase α. Those interactions are important for RPA functions such as confirming eukaryotic DNA metabolism.[18–20]

Crystal structure of RPA70N (PDB ID: 2B29) showed typical OB-fold (residues 1-120).[13] Its basic cleft located in between L12 and L45 (the loops between 1st and 2nd β-strand and 4 th and 5th β-strand) is known to interact with DNA-processing protein partners.[13,21] Tumor suppressor p53 binds to the basic cleft of RPA70N with electrostatic interaction by using acidic

* Correspondence to: **Chin-Ju Park,** Department of Chemistry, Gwangju Institute of Science and Technology, Gwangju 61005, South Korea, Tel: 062-715-3676; E-mail: cjpark@gist.ac.kr

residues of p53. Also, hydrophobic interactions between aliphatic and aromatic residues of p53 and hydrophobic floor of the RPA70N contribute to their binding.[13] This interaction of RPA70N with acidic peptide induces conformational change and chemical shift perturbation (CSP) of RPA70N.[13–15] Significantly increased CSPs at the basic cleft of RPA70N were previously observed with titration of three peptides, ATRIP, RAD9, MRE11, and BLM to RPA70N.[14,15,22-23]

Even though RPA70N contributes to critical DNA metabolisms *via* protein-protein interaction, there is no detailed information available on RPA70N dynamics. Previously, it was revealed that DNA-binding and protein interaction of RPA 70 are independent of each other. In this connection, relaxation data that was focused on the comparison of RPA70AB in absence and presence of oligonucleotides were reported.[22]

In order to understand dynamics of RPA70N relating to its protein interaction, we collected ^{15}N relaxation data and characterized several parameters of model-free analysis of human RPA70N (hRPA70N). Our results show that the L12 and L45 loops have fast timescale motions and β-barrel surfaces had rarely dynamic on both fast and intermediate timescales where ligand-binding residues are positioned at. It suggests that the binding surfaces maintain mostly rigid backbone structure for interaction with flexible partners while the binding possibly can induce the conformational change with flexible loop regions.

Experimental Methods

Sample preparation

^{15}N labeled human RPA70N was expressed and purified as described previously.[25] Final buffer was 20 mM Tris, 100 mM NaCl, 2 mM DTT at pH 7.4.

NMR spectroscopy

All NMR experiments were performed at 298 K using 900 MHz Bruker *AVANCE* II equipped with cryoprobes (Korea Basic Science Institute, Ochang). Obtained NMR data were processed using Topspin software (Bruker) and analyzed with SPARKY (T. D. Goddard and D. G. Kneller, SPARKY 3, University of California, San Francisco). ^{15}N-relaxation data were measured using delay times 10, 30, 100, 300, 500, 800, 1000, 1500 ms for longitudinal relaxation and delay times 0, 17.6, 35.2, 52.8 (x2), 88, 123.2, 176 ms for transverse relaxation. The ^{1}H-^{15}N NOE values were calculated by the ratio of peak intensities recorded with and without a ^{1}H saturation time of 10 s.[24]

Analysis of NMR-relaxation data

The backbone assignment of the protein was reported previously.[25] ^{15}N-relaxation time constants T_1 and T_2 were calculated from two-parameter single exponential fits of peak intensities versus delay times.[24] Based on this ^{15}N-relaxation data (T_1, T_2 and heteronuclear NOE), the parameters of dynamics (order parameter, local correlation time, rotational correlation time and contribution exchange factor (R_{ex}) were determined by using model-free analysis through protein dynamics software ROTDIF3.[26,27] Solution NMR PDB file of hRPA70N (PDB ID: 1EWI[21]) and its specific document form of relaxation data (T_1, T_2 and heteronuclear NOE) was required as input data. All standard error of NOE was arbitrarily given as 0.05. This program executed with full statistics optimized with running condition Robust Least-squares. All parameters of model-free analysis were extracted by axially-symmetric rotational diffusion model that was selected by minimization of chi-squared statistics and F-tests.

The spectral density functions J(ω) approximated by Bracken et *al* were calculated at $\omega = \omega_0$, ω_N and $0.87\omega_H$ from measured ^{15}N relaxation parameters (NOE, R_1, R_2).[28]

Results and Discussions

Backbone dynamics

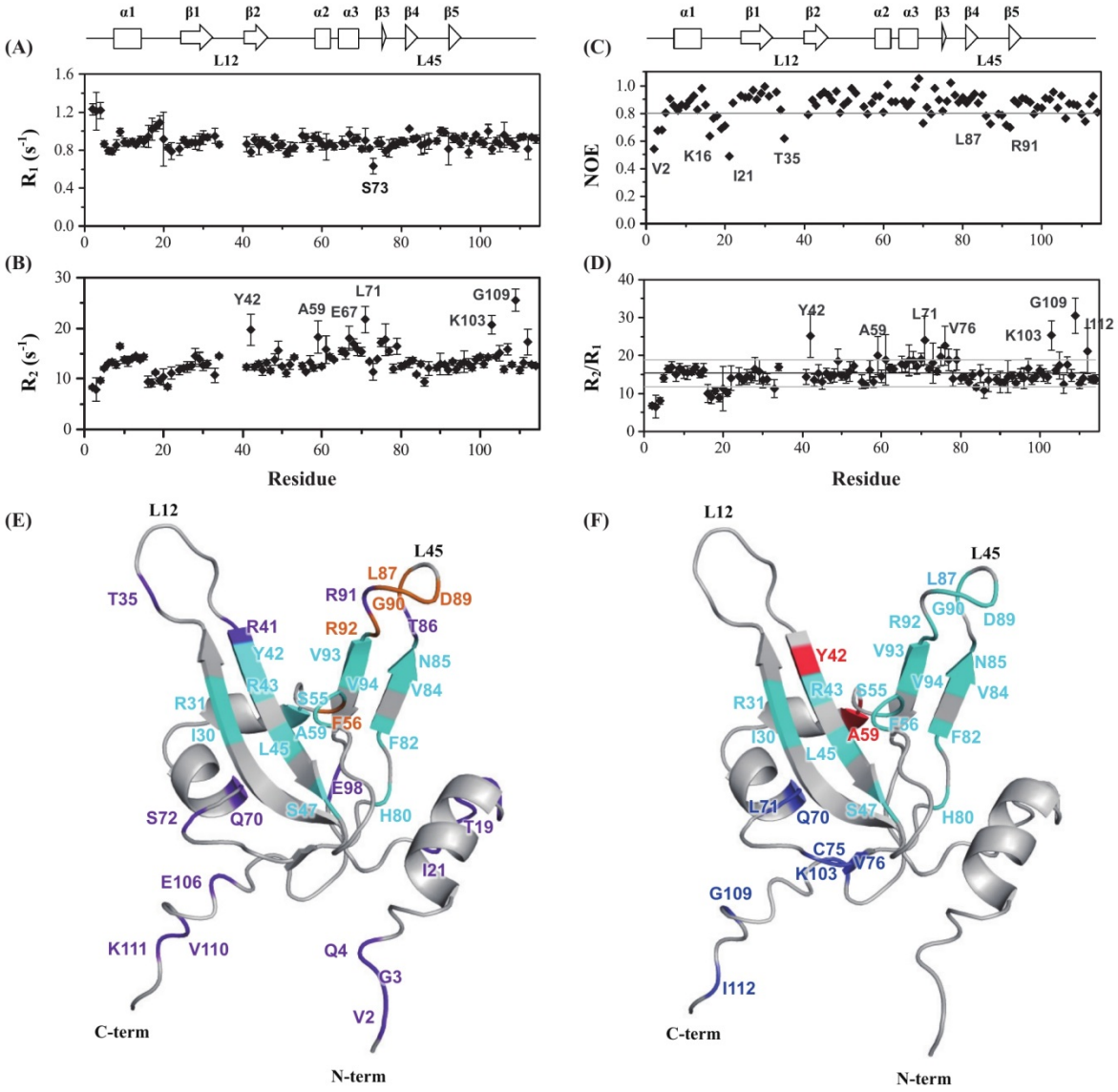

Figure 1. Observed ^{15}N-relaxation rates, **(A)** R_1 and **(B)** R_2 and **(C)** ^{1}H-^{15}N heteronuclear NOEs of hRPA70N at 900 MHz. **(D)** R_2/R_1 ratios of hRPA70N from **(A)** and **(B)**. The *Black* and two *gray solid lines* indicate average value and one standard deviation range, respectively. Mapping of **(E)** NOEs (<0.8, *purple*) and **(F)** R_2/R_1 ratios (>1SD, *blue*) with significantly perturbed regions (*cyan*) with titrated peptides onto solution secondary structure of hRPA70N (PDB ID: 1EWI[13]). Their overlapped regions were respectively shown in **(E)** *Orange* and **(F)** *Red*.

We measured ^{15}N NMR relaxation parameters, R_1, R_2 and heteronuclear NOE values of each amide bond for hRPA70N (residues 1-114) with 900 MHz NMR spectrometer. Assigned amino acids which occupied 90 percentage of full sequence of hRPA70N were assessed in relaxation parameters. The average standard error was 6.64 % for exponential-fitting of R_1 and 6.9 % for R_2. The mean values of R_1 and R_2 were 0.9 s^{-1} and 13.5 s^{-1}, and their standard deviation (SD) were 0.086 s^{-1} (9% of average R_1) and 2.676 s^{-1} (18% of average R_2), respectively. The dispersed range of R_1 was

relatively narrow and higher R_1 values were shown in N-terminal loop and α1-β1 loop (Figure 1A). On the other hand, R_2 values of loop regions were mostly low (Figure 1B). The residues those R_2 are significantly larger than 18 s^{-1} (average + 1.7 × SD) were Y42, A59, E67, L71, K103, G109 and I112 (Figure 1B). Mean value of NOE was 0.856 with its standard deviation, 0.096 (11% of average NOE), which indicates that hRPA70N is rigid overall (Figure 1C). Structured regions had high NOE values. N-terminal part and the α1-β1 loop had significantly low values correlated with their low values of R_2 (Figure 1E). On the other hand, C-terminal part had high NOE values with several high R_2 values (Figure 1B and 1C). Furthermore, NOE values of T35 in L12 and T86, L87, D89, G90, R91, and R92 in L45 loops were also relatively small. These data imply that these regions are locally flexible.

To investigate the existence of conformational exchange, we calculated R_2/R_1 ratio (Figure 1D). Several amino acids (Y42, L71, V76, K103, G109 and I112) had considerably high values of R_2/R_1 over one standard deviation (Figure 1D and 1F). This implies intermediate timescale (μs-ms) internal motions and these residues with low values of R_2/R_1 were consistent with low NOE values.

We compared those relaxation results and CSP of hRPA70N with titrated protein ligands (ATRIP, RAD9, and MRE11) previously reported (Figure 1E and 1F).[14] Among perturbed residues, L87, D89, G90, and R92 in the L45 loop and F56 of hydrophobic floor had lower NOE values than 0.8 and Y42 of β2 and A59 of α2 had higher R_2/R_1 ratio than one standard deviation (Figure 1E and 1F). This suggests most of perturbed regions on β-barrel of binding site are rigid overall and the L45 loop of basic cleft are flexible.

Model-free analysis

Based on the ^{15}N relaxation data, we characterized the dynamics of hRPA70N using model-free analysis through protein dynamics software ROTDIF to study global and local motions of each residue of hRPA70N. For selected axially-symmetric rotation diffusion model, rotational correlation time (τ_m) was estimated as 7.8 ns by following equation:

$$\tau_m = (4D_{\perp}+2D_{\parallel})^{-1} \quad (1)$$

where perpendicular rotational diffusion constant ($D_{\perp}$) and parallel rotational diffusion constant ($D_{\parallel}$) are 2.2 s^{-1} and 1.94 s^{-1}, respectively.[29-32]

In the sense of characterizing the locally flexible regions, both NOE and S^2 showed similar patterns in the graphs (Figure 1C and 2A). The mean value of S^2 of hRPA70N was 0.843, which means hRPA70N is overall restricted flexibility on fast-timescale. Similar to NOE, S^2 was also lower than 0.8 in N-terminal (V2, G3, and Q4) and α1-β1 loop (between K16 and K22) and several amino acids in other loops except C-terminal region (Figure 2A and E). Among them, V2, G3, and Q4 in N-terminal part, K16, G17, T19, and I21 in the α1-β1 loop and T86 of the L45 loop had smaller NOE values than 0.65 (Figure 2A and E). These showed flexibility of the regions on fast-timescale. Unfortunately, we could not obtain S^2 for the L12 region because of lack of the assignment and analysis. We mapped those flexible regions on solution structure of hRPA70N with significantly perturbed regions shown in Figure 2E. Y42 of β2, F56 of hydrophobic floor, V84 of β4, and R92 of the L45 loop had relatively smaller S^2 values with peak migrations in previous NMR-based titration experiments (Figure 2E).[14,15] Two amino acids, F56 and R92 were consistent with low NOE values (Figure 1E). As mentioned above, from the robust regression method, obtained values of R_{ex} are presentative in Figure 2B and compared to R_2 in Figure 2C. 26 amino acids of 112 assigned residues have conformational exchange contribution and among them, except amino acid S6, all values of R_{ex} are occupied more than 10 % of transverse rate. R_{ex}-existed amino acids were abundant between α2 and β4 (residues 59-79) and in C-terminal region and α1 (Figure 2B). Even though the values of R_{ex}

exist and contains intermediate timescale internal motions, its detailed information could not be investigated by model-free analysis. Thus, R_{ex} could not contribute to S^2 in this study. That could be confirmed on the residues K103 and G109 which had large R_{ex} values more than 40% in R_2 (Figure 2B and D). In the basic cleft, T34 of the L12 loop and L53 of the hydrophobic floor had 1.96 s^{-1} and 1.79 s^{-1} of R_{ex} with 13 % of R_2, respectively. Like R_2/R_1 ratio, Y42 and A59 were overlapped regions with intermediate dynamics and CSPs (Figure 1F and 2F).

In model-free analysis of hRPA70N, fast -timescale local motions had their period which is called as internal correlation time (τ_e). The local correlation time of hRPA70N were separated in two range of fast-timescale. The internal correlation time mostly

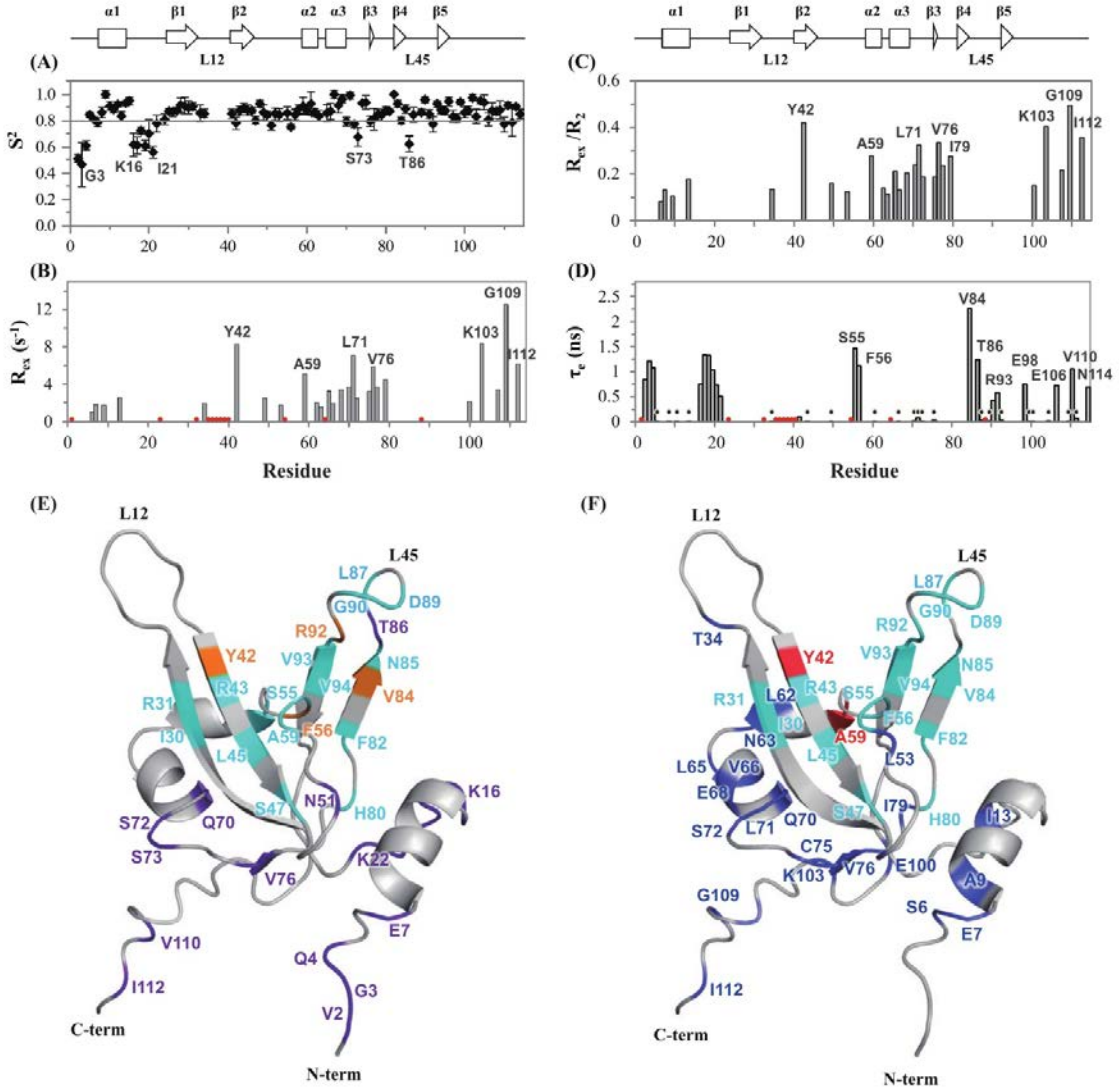

Figure 2. Obtained model-free parameters, **(A)** S^2, **(B)** R_{ex}, and **(D)** τ_e of hRPA70N from protein dynamics software program ROTDIF3. Red circle symbols in **(B)** and **(D)** indicate unassigned or not analyzed residues and black circle symbols in **(D)** indicate τ_e < 100 ps. Mapping of **(E)** S^2s (<0.8, *purple*) and **(F)** R_{ex} (*blue*) with significantly perturbed regions (*cyan*) same as **Figure 1 (E)**. Their overlapped regions were respectively shown in **(E)** *Orange* and **(F)** *Red*.

existed in loops with ns-timescale and also had ps-timescale much smaller than 100 ps, which are well-ordered on S^2 (Figure 2A and D). The several residues with ns-timescale internal correlation time were consistent with regions where S^2 values were significantly low (N-terminal, α1-β1 loop and V84 and T86 in the L45 loop, and S55 and F56 of basic cleft surface).

We compared CSPs and model-free dynamics by their mapping on solution structure of hRPA70N (Figure 2E and F). Among perturbed residues, Y42, F56, V84 and R92 had low S_2 values. Comparing with mapping of NOE and CSPs, F56 and R92 were consistent and flexibility of the L45 loop were reduced. In R_{ex}, amino acids Y42 and A59 were overlapped with perturbed regions and ratio R_2/R_1. Unlike R_2/R_1, intermediate-timescale local motions were exhibited more at α-helices which is covered around the core of hRPA70N. This indicates the binding site on β-barrel of hRPA70N were mostly rigid overall and α-helices around β-barrel had flexible mobility on intermediate-timescale, which suggests probability of their conformational change.

Reduced spectral density mapping

In order to confirm the backbone dynamics, we calculated spectral densities J(ω) of hRPA70N at $\omega = \omega_0$, ω_N and $0.87\omega_H$ from measured ^{15}N spin relaxation rates and NOE[28]. Mean value of $J(\omega_0)$ was 4.9 ns/rad with its standard deviation of 1.02 ns/rad and the pattern of the graph was very similar with R_2 (Figure 1B and 3A). The values of loops were mostly lower than average and several amino acids are larger than one standard deviation. Among them, amino acids with significantly high values were Y42, A59, E67, L71, V76, K103 and G109 and they were similar with the lists of residues with large R_2 (Figure 1B and 3A). This indicates that these residues have intermediate intramolecular dynamics[33]. Actually, amino acids, which had larger values of $J(\omega_0)$ than mean value, were abundant between α2 and β4 and C-terminal loop consistent with R_{ex} (Figure 2B and 3A).

Other spectral density function, $J(\omega_N)$ had average value of 0.22 ns/rad with its standard deviation, 0.002 ns/rad and were very restricted in a narrow range of deviation (Figure 3B). The values of N-terminal part and α1-β1 loop were significantly higher than average and only value of S73 was considerably low consistent with R_1 (Figure 1A and 3B).

Finally, the $J(0.87\omega_H)$ of three spectral density functions were also similar with relaxation parameter NOE like other two spectral density functions (Figure 1C and 3C). The average value of $J(0.87\omega_H)$ was 2.1 ps/rad and its standard deviation was 1.47 ps/rad. The structured regions had very lower values than average and significantly high values were abundant in loops. Especially, the N-terminal part, the α1-β1 loop and the L45 loop have larger values of $J(0.87\omega_H)$ than mean value of it (Figure 3C). This suggests the regions with small values of $J(0.87\omega_H)$ are rigid and well-ordered, but regions with high values have flexible mobility on fast timescale.

Conclusion

In this study, we measured ^{15}N-relaxation data of hRPA70N and reported model-free analysis and reduced spectral density mapping. The β-barrel surface which participates interactions with protein partners had rarely local motions on both fast and intermediate-timescale. On the other hand, the L45 loop and F56 in basic cleft showed fast-timescale dynamics. Based on these, we suggest that β-barrel surface of binding site is rigid overall and the fast internal motions of L45 loop enable the basic cleft loop to interact with ligands easier. Also we found that α-helices and loops around the core of hRPA70N had mostly high R_{ex}. This seems to be likely to undergo conformational change at the free state.

Acknowledgements

This work was supported by National Research Foundation (NRF) of Korea (Grant 2015R1C1A1A02036725), by a GIST Research Institute grant funded by GIST in 2017, and by the Korea Basic Science Institute under the R&D program (Project No. D37700) supervised by the Ministry of Science and ICT. We thank Mr. Sungjin Lee and Mr. Donguk Kang for their helpful discussions.

References

1. A. Georgaki, B. Strack, V. Podust, and U. Hübscher, *FEBS Lett.* **308**, 240 (1992)
2. A. Johnson and M. O'Donnell, *Annu. Rev. Biochem.* **74**, 283 (2005)
3. Y. J. Machida, J. L. Hamlin, and A. Dutta, *Cell.* **123**, 13 (2005)
4. S. K. Binz, A. M. Sheehan, and M. S. Wold, *DNA Repair (Amst).* **3**, 1015 (2004)
5. C. Iftode, Y. Daniely, and J. A. Borowiec, *Crit. Rev. Biochem. Mol. Biol.* **34**, 141 (1999)
6. M. S. Wold, *Annu. Rev. Biochem.* **66**, 61 (1997)
7. M. E. Stauffer and W. J. Chazin, *J. Biol. Chem.* **279**, 30915 (2004)
8. A. Bochkarev and E. Bochkareva, *Curr. Opin. Struct. Biol.* **14**, 36 (2004)
9. L. Zou and S.J. Elledge, *Science* **300**, 1542 (2003)
10. D. Shechter, V. Costanzo, and J. Gautier, *Nat. Cell Biol.* **6**, 648 (2004)
11. A. Yuzhakov, Z. Kelman, J. Hurwitz, and M. O'Donnell, *EMBO J.* **18**, 6189 (1999)
12. M. L. Mayer, *Nat. Struct. Mol. Biol.* **12**, 208 (2005)
13. E. Bochkareva, L. Kaustov, A. Ayed, G. -S. Yi, Y. Lu, A. P. -Lucena, J. C. C. Liao, A. L. Okorokov, J. Milner, C. H. Arrowsmith, and A. Bochkarev, *Proc.Natl. Acad. Sci.* **102**, 15412 (2005)
14. X. Xu, S. Vaithiyalingam, G. G. Glick, D. A. Mordes, W. J. Chazin, and D. Cortez, *Mol. Cell. Biol.* **28**, 7345 (2008)
15. H. L. Ball, M. R. Ehrhardt, D. A. Mordes, G. G. Glick, W. J. Chazin, and D. Cortez, *Mol. Cell. Biol.* **27**, 3367 (2007)
16. G. Mer, A. Bochkarev, R. Gupta, E. Bochkareva, L. Frappier, C. J. Ingles, A. M. Edwards, and W. J. Chazin, *Cell* **103**, 449 (2000)
17. D. L. Theobald, R. M. Mitton-Fry, and D. S. Wuttke, *Annu. Rev. Biophys. Biomol. Struct.* **32**, 115 (2003)
18. E. Bochkareva, S. Korolev, S. P. Lees-Miller, and A. Bochkarev, *EMBO J.* **21**, 1855 (2002)
19. E. Bochkareva, V. Belegu, S. Korolev, and A. Bochkarev, *EMBO J.* **20**, 612 (2001)
20. G. W. Daughdrill, J. Ackerman, N. G. Isern, M. V. Botuyan, C. Arrowsmith, M. S. Wold, and D. F. Lowry, *Nucleic Acids Res.* **29**, 3270 (2001)
21. D. M. Jacobs, A. S. Lipton, N. G. Isern, G. W. Daughdrill, D. F. Lowry, X. Gomes, and M. S. Wold, *J. Biomol. NMR* **14**, 321(1999)
22. C. A. Brosey, S. E. Soss, S. Brooks, C. Yan, I. Ivanov, K. Dorai, and W. J. Chazin, *Struct. Des.* **23**, 1028 (2015)
23. D. Kang, S. Lee, K.-S. Ryu, H.-K.Cheong, E.-H. Kim, and C.-J.Park, *FEBS Lett.* **592**, 547 (2018).
24. J.-J. Yi, W.-J. Kim, J.-K. Rhee, J. Lim, B.-J. Lee, and W.S.Son, *J. Kor. Magn. Reson. Soc.* **21**, 26 (2017)
25. S. Lee and C.-J. Park, *J. Kor. Magn. Reson. Soc.* **20**, 138 (2016)
26. O. Davulcu, Y. Peng, R. Brüschweiler, J. J. Skalicky, and M. S. Chapman, *J. Struct. Biol.* **200**, 258 (2017)
27. K. Berlin, A. Longhini, T. K. Dayie, and D. Fushman, *J. Biomol. NMR* **57**, 333 (2013)
28. C. Bracken, P. a Carr, J. Cavanagh, and A. G. Palmer, *J. Mol. Biol.* **285**, 2133 (1999)

29. D. E. Woessner, *J. Chem. Phys.* **37**, 647 (1962)
30. W. T. Huntress, *J. Chem. Phys.* **48**, 3524 (1968)
31. P. S. Hubbard, *J. Chem. Phys.* **53**, 985 (1970)
32. N. A. Farrow, O. Zhang, A. Szabo, D. A. Torchia, and L. E. Kay, *J. Biomol. NMR* **6**, 153 (1995)
33. J.-F. Lefèvre, K. T. Dayie, J. W. Peng, and G. Wagner, *Biochemistry* **35**, 2674 (1996)